

Homogeneous aerosol freezing in the tops of high-altitude tropical cumulonimbus clouds

E. J. Jensen¹ and A. S. Ackerman²

Received 11 October 2005; revised 7 March 2006; accepted 13 March 2006; published 20 April 2006.

[1] Numerical simulations of deep, intense continental tropical convection indicate that when the cloud tops extend more than a few kilometers above the liquid water homogeneous freezing level, ice nucleation due to freezing of entrained aqueous sulfate aerosols generates large concentrations of small crystals (diameters less than $\approx 20 \mu\text{m}$). The small crystals produced by aerosol freezing have the largest impact on cloud-top ice concentration for convective clouds with strong updrafts but relatively low aerosol concentrations. An implication of this result is that cloud-top ice concentrations in high anvil cirrus can be controlled primarily by updraft speeds in the tops of convective plumes and to a lesser extent by aerosol concentrations in the uppermost troposphere. While larger crystals precipitate out and sublimate in subsaturated air below, the population of small crystals can persist in the saturated uppermost troposphere for many hours, thereby prolonging the lifetime of remnants from anvil cirrus in the tropical tropopause layer. **Citation:** Jensen, E. J., and A. S. Ackerman (2006), Homogeneous aerosol freezing in the tops of high-altitude tropical cumulonimbus clouds, *Geophys. Res. Lett.*, 33, L08802, doi:10.1029/2005GL024928.

1. Introduction

[2] Deep convection in the tropics generates anvil cirrus that covers vast areas [Salby *et al.*, 1991] and significantly affects the Earth's radiation budget [Kiehl and Ramanathan, 1990]. The concentrations and sizes of ice crystals in these clouds affect the reflection of incoming solar radiation: for a given ice water content, a cloud with smaller, more numerous crystals will have a higher albedo. In addition, small crystals in anvil cirrus will tend to persist while larger crystals fall out and sublimate at lower levels.

[3] The inaccessibility of these high clouds has limited sampling of their microphysical composition. Research aircraft have typically been unable to reach the tops of tropical anvil cirrus that can extend up to $\approx 18 \text{ km}$. However, during the Stratosphere Troposphere Exchange Project (STEP), the NASA ER-2 did provide in situ measurements in high anvil cirrus in the tropical western Pacific. FSSP-100 (Forward Scattering Spectrometer Probe) measurements in anvils as high as 18 km indicated very large concentrations ($10\text{--}100 \text{ cm}^{-3}$) of relatively small ice crystals (mean mass diameters less than about $20\text{--}40 \mu\text{m}$) [Knollenberg *et al.*, 1993]. Knollenberg *et al.* [1993] speculated that rampant ice

nucleation due to homogeneous freezing of sulfate aerosols at high altitude might explain the large ice concentrations. It should be noted that persistent skepticism remains concerning the concentrations of small crystals in ice clouds inferred from instruments such as FSSP-100 given, the potential for shattering of crystals at the inlet.

[4] In recent years, satellite visible and infrared radiance measurements have been used to retrieve cloud-top effective diameters. Retrievals from AVHRR (Advanced Very High Resolution Radiometer) measurements indicate effective diameters (D_{eff}) at the tops of tropical cumulonimbus are typically on the order of $60\text{--}70 \mu\text{m}$ [Sherwood, 2002a, 2002b]. MODIS (Moderate Resolution Imaging Spectroradiometer) retrievals of anvil cirrus effective diameters give similar values. However, Sherwood *et al.* [2006] recently argued that the angular dependence of the AVHRR $3.7 \mu\text{m}$ radiance provides evidence for a population of very small crystals at the tops of tropical cumulonimbus in addition to the crystals producing $60\text{--}70 \mu\text{m}$ diameter effective diameters. They could reproduce the observed angular dependence by assuming that 35–40% of the scattering is caused by crystals with diameters of about $20 \mu\text{m}$.

[5] A recent modeling and observational study provided evidence that activation of aerosols entrained into convective updrafts in the mid-troposphere and subsequent homogeneous freezing of the droplets might control ice crystal production in subtropical deep convection [Fridlind *et al.*, 2004]. In this study, we use numerical simulations of cumulonimbus clouds in the deep tropics to demonstrate the importance of ice nucleation due to homogeneous freezing of aerosols entrained into convective updrafts in the uppermost troposphere. We show that this mechanism can dominate the ice crystal concentrations at the tops of high tropical anvil cirrus and affect the lifetime of residual anvil cirrus near the tropopause.

2. Model Description and Initialization of Simulations

[6] For our simulations, we use DHARMA (Distributed Hydrodynamic Aerosol-Radiation-Microphysics Application), a three-dimensional cloud model that simulates the coupling between atmospheric dynamics, cloud microphysics, and radiation on an Eulerian grid [Ackerman *et al.*, 2000]. The dynamical component of DHARMA is a massively-parallel, large-eddy simulation code [Stevens and Bretherton, 1996; Stevens *et al.*, 2002]. Embedded within this dynamics code is a detailed microphysical model, CARMA (Community Aerosol-Radiation-Microphysics Application) [Ackerman *et al.*, 1995; Jensen *et al.*, 1998; Fridlind *et al.*, 2004]. Aerosols, water drops, graupel, and snow are each tracked in 24 size bins, spanning 5 nm to $1 \mu\text{m}$

¹NASA Ames Research Center, Moffett Field, California, USA.

²NASA Goddard Institute for Space Studies, New York, New York, USA.

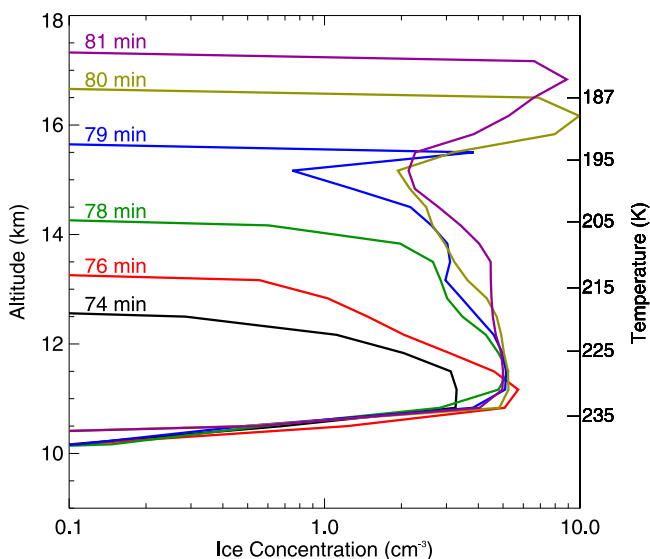


Figure 1. Height profiles of mean in-cloud ice concentration are shown for a series of times as the cloud top rises through the upper troposphere. Aerosol freezing ice nucleation occurs at 79–80 min.

for aerosols and $1\ \mu\text{m}$ to $1.2\ \text{cm}$ equivalent-volume radius for cloud hydrometeors. Radiation is treated in a two-stream calculation [Toon *et al.*, 1989] for each model column by dividing solar and infrared radiation into 26 and 18 respective wavelength bins and using Mie theory to calculate particle single-scattering properties. A wide range of microphysical processes are treated, including condensational growth, evaporation, sedimentation, melting, gravitational collection, drop breakup, homogeneous and heterogeneous freezing of aerosols and drops [Koop *et al.*, 2000], and Hallett-Mossop rime splintering.

[7] In simulations using a variety of thermodynamic soundings and surface heat fluxes, we find that whenever deep convection extends more than a few kilometers above the droplet homogeneous freezing level (about 236 K), the uppermost part of the updraft becomes depleted of ice crystals such that supersaturation rises and sporadic homogeneous freezing of entrained sulfate aerosols generates large numbers of small crystals. Here, we show results from an exemplary set of simulations to demonstrate the importance of aerosol freezing.

[8] The initial thermodynamic state for the simulations is based on the 18 November 2001 02:15 UTC sounding launched at Darwin, Australia during DAWEX (Darwin Area Wave Experiment) [Tsuda *et al.*, 2004]. The Väisälä RS80 soundings do not reliably measure relative humidity in the cold upper troposphere. The error in the DAWEX soundings is clearly evident as a smooth relative humidity dropoff above 15 km. We adjusted the sounding such that the relative humidity with respect to ice increased to 130% in the tropopause region, as is typically observed in the tropics by frostpoint soundings and aircraft measurements [Kley *et al.*, 1997; Jensen *et al.*, 2001]. The convective available potential energy for this sounding is $2.6\ \text{kJ kg}^{-1}$. Open boundary conditions are used at each of the horizontal faces, with a cosine-squared forcing function used to nudge fields toward the initial sounding. Convection is triggered

by specifying sensible and latent surface heat fluxes of $500\ \text{W m}^{-2}$ each over a 6 km radius area in the center of the $48 \times 48\ \text{km}$ horizontal domain. The grid resolution is 500 m in the horizontal and 375 m in the vertical, with a vertical domain of 0 to 24 km. To avoid advection of anvil cirrus out of the domain, we translate the grid after 3 hours at a rate equal to the upper tropospheric winds (a few m s^{-1}).

[9] For our baseline simulation, we specify height-dependent lognormal aerosol size distribution parameters corresponding to relatively low aerosol loading. Specifically, we attempted to match the lower envelope of aerosol concentration, surface area, and volume given by Clarke and Kapustin [2002, Figure 14]. Aerosol concentrations range from $100\ \text{cm}^{-3}$ in the boundary layer to $900\ \text{cm}^{-3}$ near the tropopause; mode radius is specified as 60 nm in the boundary layer decreasing to 30 nm near the tropopause; and geometric standard deviation ranges from 1.3 to 1.5.

[10] To evaluate the impact of aqueous aerosol freezing, we compare a baseline simulation with this process included to a simulation with this process shut off. Sensitivity tests are used to evaluate the importance of aerosol freezing given different aerosol concentrations, updraft speeds, and ice crystal aggregation rates.

3. Results

[11] In the baseline continental convection cases, the surface heat fluxes imposed trigger deep, strong convection with updraft speeds as high as $30\text{--}40\ \text{m s}^{-1}$ developing about an hour into the simulation. The cloud top reaches the tropopause region (17–18 km) within 90 min. Heterogeneous ice nucleation generates small concentrations of ice crystals ($<0.1\ \text{cm}^{-3}$) at altitudes between about 5 and 10 km, but most cloud droplets reach the homogeneous freezing level at about 10 km wherein rapid droplet freezing produces ice concentrations as high as about $5\ \text{cm}^{-3}$. As the cloud top rises further through the upper troposphere, ice nucleation occurs again at about 79–80 min (see Figure 1) when the ice concentration near cloud top has decreased sufficiently to allow supersaturation to build up to the point where aqueous sulfate aerosols homogeneously freeze. Given the rapid cooling driven by strong convective updrafts, large numbers of ice crystals are generated in these nucleation events ($\approx 5\text{--}10\ \text{cm}^{-3}$). Note that the ice concentrations in Figure 1 are horizontally averaged, and peak ice concentrations in the updraft cores exceed $40\ \text{cm}^{-3}$.

[12] The mature anvil generated by the simulated convection extends above 17 km. Nucleation of ice by aerosol freezing in the uppermost troposphere (above $\approx 15\ \text{km}$) results in a bimodal ice crystal size distribution near the anvil top (see Figure 2). Numerous small crystals with diameters less than $\approx 20\ \mu\text{m}$ are present along with a population of larger crystals. The small crystals are absent in the simulation without aerosol freezing. Note that D_{eff} increases rapidly with distance below cloud top. The satellite D_{eff} retrievals represent approximately the first two optical depths into the cloud top [Platnick, 2000] (a few km for the simulated anvil cirrus). The cloud-top effective diameters averaged over the top few kilometers of the cloud ($\approx 60\text{--}70\ \mu\text{m}$) agree well with AVHRR and MODIS retrievals. (We use the standard definition of D_{eff} as the ratio of the third and second moments of the size distribu-

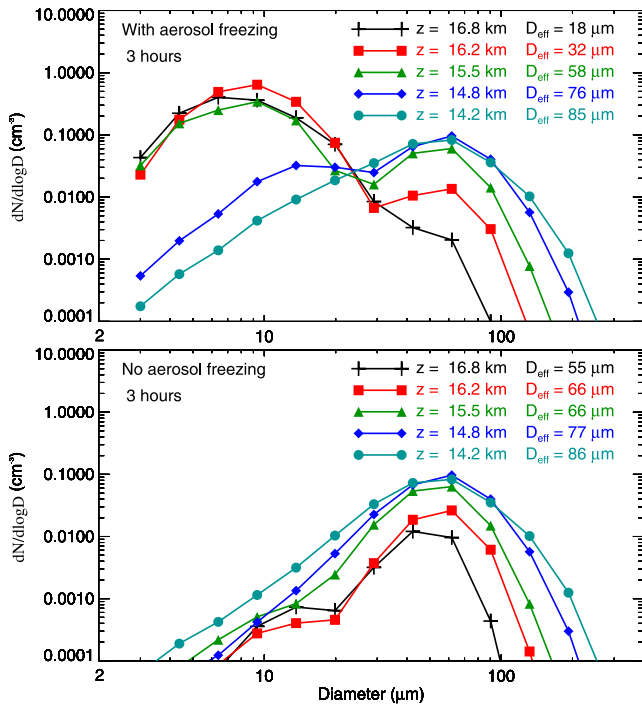


Figure 2. Horizontally averaged ice crystal size distributions at the tops of anvil cirrus generated by deep convection at 3 hours into the simulation. (top) Baseline simulation with aerosol freezing; (bottom) no aerosol freezing.

tion.) The effective diameter in the simulated clouds is dominated by the large crystal mode.

[13] In the simulated convective cores, activation of droplets depletes the initial $\approx 100 \text{ cm}^{-3}$ aerosol concentration to less than 10 cm^{-3} in the low-mid troposphere. However, at the highest levels in the convective updrafts, the aerosol concentration builds up again to nearly 600 cm^{-3} as entrainment of ambient upper tropospheric air brings in a fresh population of aerosols. Hence, there is an ample supply of aerosols for homogeneous freezing ice nucleation, and most of these aerosols are entrained into the plumes in the upper troposphere. Even without entrainment of aerosols above 10 km, there are still enough aerosols remaining in the convective cores to produce significant ice concentrations via aerosol freezing. However, the entrained aerosols are generally larger than the small aerosols remaining after droplet activation at lower levels, and the larger entrained aerosols are the ones that freeze.

[14] Note that the aerosol freezing process here is selective, just as it is in cirrus clouds formed in situ in the upper troposphere. In other words, only a fraction of the aerosols freeze, and that fraction depends primarily on the cooling rate [Jensen and Toon, 1994; Kärcher and Lohmann, 2002]. In the baseline simulation shown here, only aerosols with radii larger than about $0.1 \mu\text{m}$ freeze. With stronger (weaker) updrafts in the upper troposphere, larger (smaller) ice concentrations are produced. However, since the cooling in convective updrafts is very rapid, and the ice nucleation is occurring under cold conditions, the concentration of ice crystals produced is moderately sensitive to aerosol concentration, as demonstrated by modeling studies [Jensen and Toon, 1994; Kärcher and Lohmann, 2002].

[15] We have run a number of sensitivity tests to evaluate the robustness of these results with respect to uncertainties in physical processes and environmental conditions. Ice crystal aggregation efficiencies are not well known, particularly at very low temperatures. Even with the ice-ice aggregation process entirely shut off in the model, cloud-top ice concentrations still decrease in the rising plume, allowing pulses of aerosol freezing in the upper troposphere. With the initial aerosol concentration profile increased by a factor of 5 (approximating the heavy aerosol loading conditions given by Clarke and Kapustin [2002, Figure 14]), we still get production of small crystals by aerosol freezing near cloud top, but these crystals do not dominate the ice concentration. The baseline simulation, with the Darwin sounding and $30\text{--}40 \text{ m s}^{-1}$ updrafts, was clearly a continental convection case. We have also run maritime convection simulations using soundings from the CEPEX (Central Equatorial Pacific Experiment) cruise. Aerosol freezing still

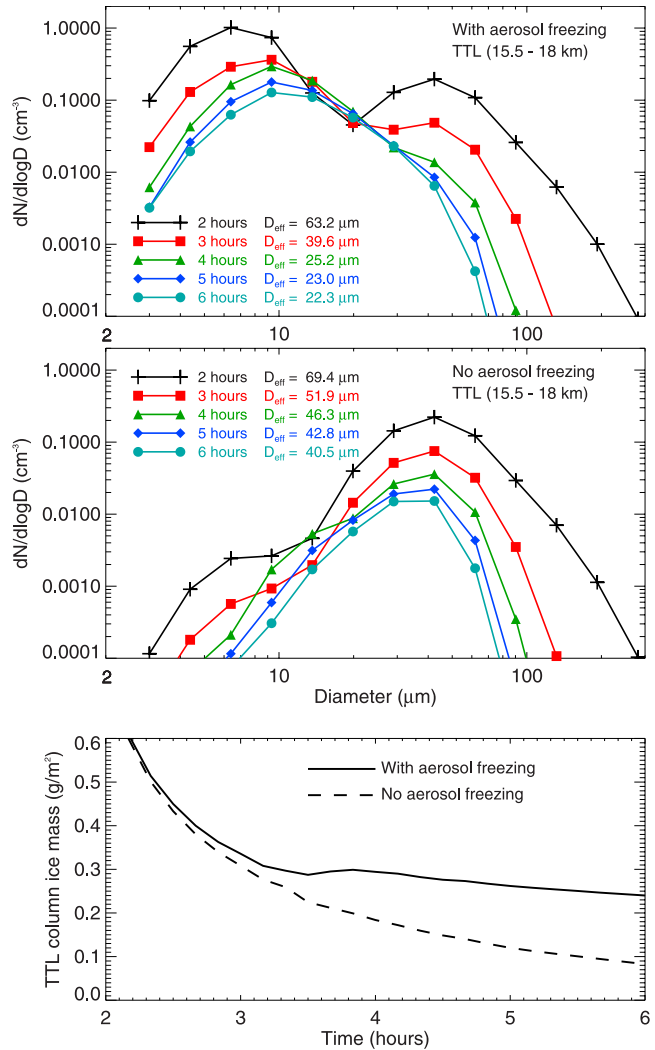


Figure 3. Horizontally and vertically averaged ice crystal size distributions in the tropical tropopause layer (15.5–18 km) in simulations (top) with and (middle) without aerosol freezing. (bottom) The evolution of column TTL ice mass in the two simulations (total ice mass divided by horizontal domain area).

occurs in the tops of the 10–20 m s⁻¹ maritime convective updrafts, but the ice concentrations produced are considerably lower than in the continental convection simulations and do not dramatically increase the cloud-top ice concentration. Hence, the aerosol freezing process has the largest relative impact on cloud-top ice concentration in continental convection with relatively low aerosol concentrations in the lower troposphere.

[16] The amount of ice lofted to the tropical tropopause layer (TTL) by the initial convection is not affected by the aerosol freezing process, but the ice crystals generated from aerosol freezing strongly impact the evolution of the uppermost part of the cloud (Figure 3). In the simulation with aerosol freezing, about half of the TTL ice mass is in crystals small enough such that they remain in the TTL throughout the 6-hour simulation. After 4 hours, the ice crystal effective diameter and total ice mass decrease relatively slowly with time. In contrast, the large crystals lofted into the TTL in the simulation without aerosol freezing rapidly settle out such that very little ice mass remains at 6 hours.

[17] Several studies have suggested that much of the widespread thin cirrus in the TTL has its origins in deep convection. *Massie et al.* [2002] used trajectory analysis to show that half of the TTL thin cirrus observed by HALOE (Halogen Occultation Experiment) could be leftover from convective injection. *Pfister et al.* [2001] argued that the structured TTL cirrus observed with airborne lidar measurements originated from deep convection. The global GLAS (Geoscience Laser Altimeter System) measurements show that the regions with the highest frequencies of TTL thin cirrus are approximately collocated with regions having frequent deep convection [*Dessler et al.*, 2006]. The simulations presented here suggest that most of the ice crystals in such persistent, convectively generated TTL cirrus are nucleated by homogeneous freezing of aerosols near the tops of convective updrafts, and without this process the convectively generated TTL thin cirrus would be far less prevalent.

[18] **Acknowledgment.** This work was supported by NASA's Radiation Science Program and the Department of Energy Atmospheric Radiation Program.

References

- Ackerman, A. S., O. B. Toon, and P. V. Hobbs (1995), A model for particle microphysics, turbulent mixing, and radiative transfer in the stratocumulus-topped marine boundary layer and comparisons with measurements, *J. Atmos. Sci.*, *52*, 1204–1236.
- Ackerman, A. S., O. B. Toon, D. E. Stevens, A. J. Heymsfield, V. Ramanathan, and E. J. Welton (2000), Reduction of tropical cloudiness by soot, *Science*, *288*, 1042–1047.
- Clarke, A. D., and V. N. Kapustin (2002), A Pacific aerosol survey. part I: A decade of data on particle production, transport, evolution, and mixing in the troposphere, *J. Atmos. Sci.*, *59*, 363–382.
- Dessler, A. E., S. P. Palm, W. D. Hart, and J. D. Spinhirne (2006), Tropopause-level thin cirrus coverage revealed by ICESat/Geoscience Laser Altimeter System, *J. Geophys. Res.*, doi:10.1029/2005JD006586, in press.
- Fridlind, A. M., et al. (2004), Evidence for the predominance of mid-tropospheric aerosols as subtropical anvil nuclei, *Science*, *303*, 718–722.
- Jensen, E. J., and O. B. Toon (1994), Ice nucleation in the upper troposphere: Sensitivity to aerosol number density, temperature, and cooling rate, *Geophys. Res. Lett.*, *21*, 2019–2022.
- Jensen, E. J., A. S. Ackerman, D. E. Stevens, O. B. Toon, and P. Minnis (1998), Spreading and growth of contrails in a sheared environment, *J. Geophys. Res.*, *103*, 31,557–31,569.
- Jensen, E. J., L. Pfister, A. S. Ackerman, A. Tabazadeh, and O. B. Toon (2001), A conceptual model of the dehydration of air due to freeze-drying by optically thin, laminar cirrus rising slowly across the tropical tropopause, *J. Geophys. Res.*, *106*, 17,273–17,252.
- Kärcher, B., and U. Lohmann (2002), A parameterization of cirrus cloud formation: Homogeneous freezing of supercooled aerosols, *J. Geophys. Res.*, *107*(D2), 4010, doi:10.1029/2001JD000470.
- Kiehl, J. T., and V. Ramanathan (1990), Comparison of cloud forcing derived from the Earth Radiation Budget Experiment with that simulated by the NCAR Community Climate Model, *J. Geophys. Res.*, *95*, 11,679–11,698.
- Kley, D., H. G. Smit, H. Vömel, H. Grassl, V. Ramanathan, P. J. Crutzen, S. Williams, J. Meywerk, and S. J. Oltmans (1997), Tropospheric water vapour and ozone cross-sections in a zonal plane over the central equatorial Pacific Ocean, *Quart. J. R. Meteorol. Soc.*, *123*, 2009–2040.
- Knollenberg, R. G., K. Kelly, and J. C. Wilson (1993), Measurements of high number densities of ice crystals in the tops of tropical cumulonimbus, *J. Geophys. Res.*, *98*, 8639–8664.
- Koop, T., B. Luo, A. Tsias, and T. Peter (2000), Water activity as the determinant for homogeneous ice nucleation in aqueous solutions, *Nature*, *406*, 611–614.
- Massie, S., A. Gettelman, W. Randel, and D. Baumgardner (2002), Distribution of tropical cirrus in relation to convection, *J. Geophys. Res.*, *107*(D21), 4591, doi:10.1029/2001JD001293.
- Pfister, L., et al. (2001), Aircraft observations of thin cirrus clouds near the tropical tropopause, *J. Geophys. Res.*, *106*, 9765–9786.
- Platnick, S. (2000), Vertical photon transport in cloud remote sensing problems, *J. Geophys. Res.*, *105*, 22,919–22,935.
- Salby, M. L., H. H. Hendon, K. Woodberry, and K. Tanaka (1991), Analysis of global cloud imagery from multiple satellites, *Bull. Am. Meteorol. Soc.*, *72*, 467–480.
- Sherwood, S. C. (2002a), Aerosols and ice particle size in tropical cumulonimbus, *J. Clim.*, *15*, 1051–1062.
- Sherwood, S. C. (2002b), Corrigendum, *J. Clim.*, *15*, 3727.
- Sherwood, S. C., V. T. P. Phillips, and J. S. Wettlaufer (2006), Small Ice Crystals and the Climatology of Lightning, *Geophys. Res. Lett.*, *33*, L05804, doi:10.1029/2005GL025242.
- Stevens, D. E., and C. S. Bretherton (1996), A forward-in-time advection scheme and adaptive multilevel flow solver for nearly incompressible atmospheric flow, *J. Comput. Phys.*, *129*, 284–289.
- Stevens, D. E., A. S. Ackerman, and C. S. Bretherton (2002), Effects of domain size and numerical resolution on the simulation of shallow cumulus convection, *J. Atmos. Sci.*, *59*, 3285–3301.
- Toon, O. B., C. P. McKay, T. P. Ackerman, and K. Santhanam (1989), Rapid calculation of radiative heating rates and photodissociation rates in inhomogeneous multiple scattering atmospheres, *J. Geophys. Res.*, *94*, 16,287–16,301.
- Tsuda, T., M. V. Ratnam, P. T. May, M. J. Alexander, R. A. Vincent, and A. MacKinnon (2004), Characteristics of gravity waves with short vertical wavelengths observed with radiosonde and GPS occultation during DAWEX (Darwin Area Wave Experiment), *J. Geophys. Res.*, *109*, D20S03, doi:10.1029/2004JD004946.

A. S. Ackerman, NASA Goddard Institute for Space Studies, 2880 Broadway, New York, NY 10025, USA. (andrew.ackerman@nasa.gov)

E. J. Jensen, NASA Ames Research Center, Moffett Field, CA 94035, USA. (eric.j.jensen@nasa.gov)